



Power enhancement in PV arrays under partial shaded conditions with different array configuration

Sakthivel Ganesan^a, Prince Winston David^a, Praveen Kumar Balachandran^{b,*}, Ilhami Colak^c

^a Department of Electrical and Electronics Engineering, Kamaraj College of Engineering and Technology, Tamilnadu, India

^b Department of Electrical and Electronics Engineering, Vardhaman College of Engineering, Telangana, India

^c Department of Electrical and Electronics Engineering, Faculty of Engineering and Architectures, Nisantasi University, 34398, Istanbul, Turkey

ARTICLE INFO

Keywords:

Photovoltaic array
Reconfiguration
Partial shading
Mismatch loss

ABSTRACT

Solar Photovoltaic systems are used for electrical power generation, and they provide an alternative source to non-renewable energy sources like coal, oil, natural gas and nuclear energy. Photovoltaic arrays used in PV systems may be subjected to partial shading conditions, thereby affecting power generation because of higher power mismatch losses. Due to an uneven distribution of irradiation condition, some of the bypass diodes turned on and affect the power generation in a photovoltaic array. The mismatch losses are due to the output from PV panels subjected to different irradiances because of non-uniform partial shading conditions. The power loss can be reduced by uniformly distributing the partially shaded condition over the entire PV array. In this work different shaped 4×4 array configuration is proposed to overcome the effect of partial shading condition, thereby providing lower mismatch losses. Simulations under different partial shading conditions are carried out using MATLAB Simulink, and the experimental setups carried out for the proposed array configuration for 4×4 PV array and the results are discussed.

1. Introduction

In the globe, the electricity generating systems are changing continuously in order to meet out the increase in power demand and also much importance is given for the reduction in emission of greenhouse gases. Using renewable energy sources like solar energy and wind energy helps generate electrical power with lower carbon dioxide emissions [1]. Among the existing different renewable technologies in power generation, solar PV system has the capability of generating clean and reliable electrical power in future. In the world, government is taking several measures for power generation using solar energy by providing grants. Due to the tremendous improvement in PV technology, around 512 GW power is generated using solar energy in 2018. The installation cost of PV system is getting reduced day by day, demonstrating the commitment to the effective use of solar power [2].

Power generation from the PV panels mainly depends on atmospheric conditions and also non-linear characteristics makes it very difficult in increasing the overall efficiency. There are also several factors that reduce the power generation from PV arrays. One such factor is partial shading due to shadows from the building, dust, dropping from the bird and ageing of PV panels [3–6]. The partial

* Corresponding author.

E-mail addresses: sakthissg@gmail.com (S. Ganesan), dpwtce@gmail.com (P.W. David), praveenbala038@gmail.com (P.K. Balachandran), ilhcol@gmail.com (I. Colak).

<https://doi.org/10.1016/j.heliyon.2024.e23992>

Received 12 July 2023; Received in revised form 21 December 2023; Accepted 2 January 2024

Available online 11 January 2024

2405-8440/© 2024 The Authors. Published by Elsevier Ltd. This is an open access article under the CC BY-NC-ND license (<http://creativecommons.org/licenses/by-nc-nd/4.0/>).

shading effects on PV arrays can be minimised by providing proper distribution of shading in the surface of PV array by arranging and connecting them in various different configurations.

Based on this different configuration like series parallel connection, Bridge link connection, Total cross tied connection, Honey comb connections are carried out for PV array [7–17]. To analyse the reliability behaviour of large PV of array size 720 × 20, they are connected in three different connections like series-parallel, total cross tied and bridge link connections and proved the lifetime in TCT connection is 30 % more when compared to other connections [18]. Similarly, authors investigated for 6 × 6 PV array in different configurations and different irradiance pattern. If the PV array has the panels are connected in series connection and they are subjected to shading conditions results the reduction of current in the entire PV array and they are only suitable for very low shading environment conditions. The parallel connection need more components comparing to series parallel connection, bridge link connection, honey comb connection and Total cross tied connection the latter one has provided better power enhancement under any shaded conditions [19–23]. The series parallel connection is complex to design and install and also string balancing is critical,

In general, the output power is getting reduced on the load side due to the following factors. 1. Short circuit 2. hotspot 3. Partial shading condition, and [24]diode failure. Earlier many research work carried out to reduce the effect of partial shading. To reduce the impact bypass diode method is used [25–27]. In this method the output power at the load is only due to unshaded PV cells whereas the shaded PV cells are bypassed. This method is not useful for extracting maximum power due to separation of shaded PV cells in an array. From the P–V Characteristic curve, the point at which maximum power can be generated can be found out. But partial shaded condition leads to local maximum power points. MPPT algorithms like Perturb and Observe and Incremental Conductance are used to generate maximum power by changing the operating points. This makes difficult in achieving global maximum MPPT. When compared to conventional methods, optimization algorithm along with MPPT has more efficiency but it also failed in some cases [28–30]. The power can be enhanced by changing the physical interconnection between the PV modules. Fig. 1 a shows the matrix configuration diagram of 4 × 4 PV array. Fig. 1 b shows 4 × 4 PV modules connected in TCT configuration, the parameters and rating of the modules are listed in Table 1.

The equivalent circuit of PV cell is shown in Fig. 2. PV cell consists of current source I connected in parallel with the diode D, resistance R_{sh} and in series with resistance R_{se}. I represent the Photocell current, R_{sh}represents shunt resistance, R_{se}represents series resistance and I_d represents diode current. Applying Kirchoff’s Current law, the current entering in the node is given by

$$I_{pv} = I - I_d - I_{sh} \tag{1}$$

$$I = I_{ph} - I_d [-\exp(V + R_s + I_{pv})/A) - 1] - [(V_{pv} + R_s I_{pv})/R_{sh}] \tag{2}$$

2. Proposed array configuration

The proposed array configuration is listed in Table 2.

3. Algorithm of the proposed work

The algorithm of the proposed work is shown in Fig. 3 and also written in detail below.

3.1. Algorithm

Step 1. Enter the number of “m” rows and “n” columns of the PV array.

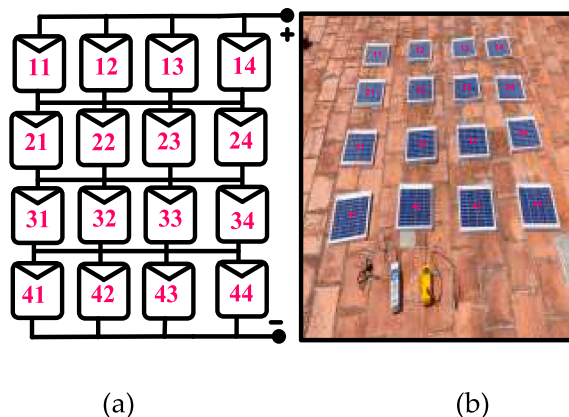


Fig. 1. a 4 × 4 matrix Solar PV array 1. b TCT configuration.

Table 1
Specifications of PV module.

Parameters and Module rating of PV array	
Voltage at peak power V_m -20V	Current at Peak Power I_m -0.5A
Open circuit voltage V_{oc} -24.8V	Short circuit current I_{sc} -0.6A

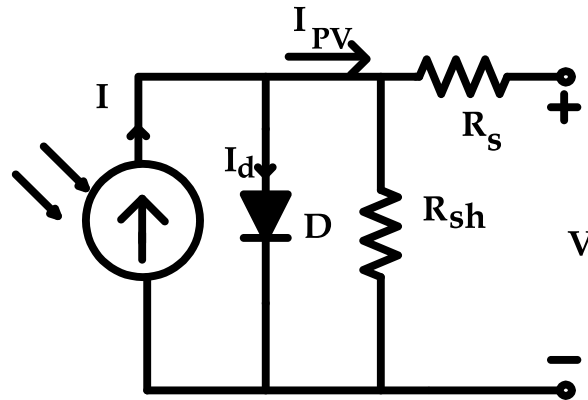


Fig. 2. Equivalent circuit of PV cell.

Table 2
Proposed array configuration.

Configuration	1.	2.	3.	4.	5.	6.	7.	8.	9.	10.	11.
Pattern	Z	↘	X	○	=	□	L	<	>	└	*

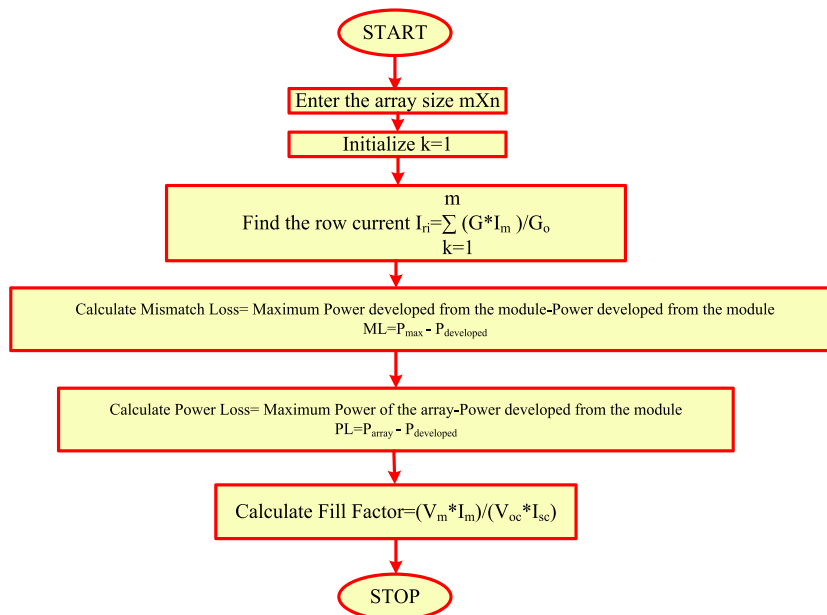


Fig. 3. Flow chart of the proposed work.

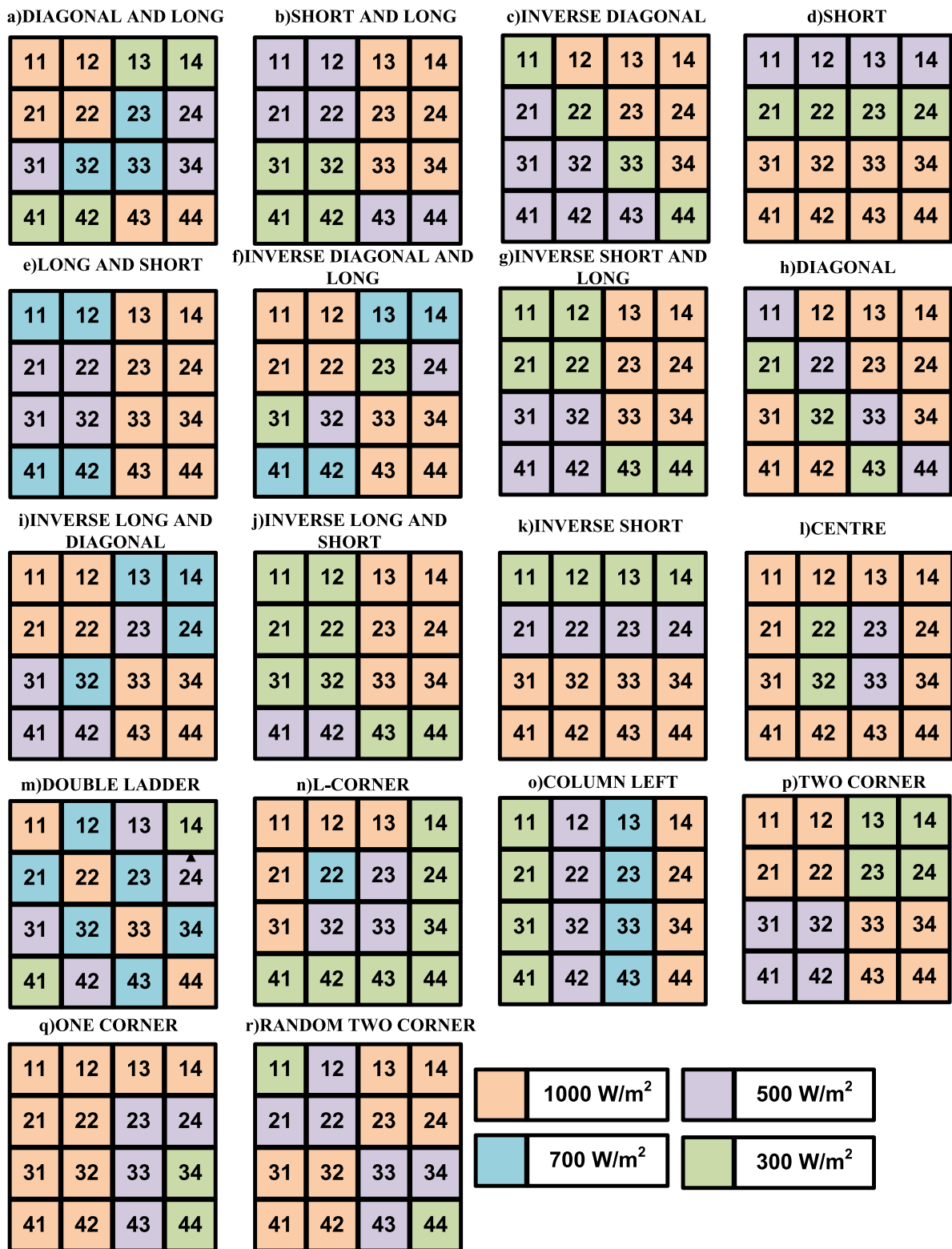


Fig. 4. Shading pattern in the PV array a) Diagonal and long b) short and long c) inverse diagonal d) short e) long and short f) Inverse diagonal and long g) Inverse short and long h) diagonal i) Inverse long and diagonal j) Inverse long and short k) Inverse short l) centre m) double ladder n) L-Corner o) Column left p) Two corner q) One corner r) Random two corner.

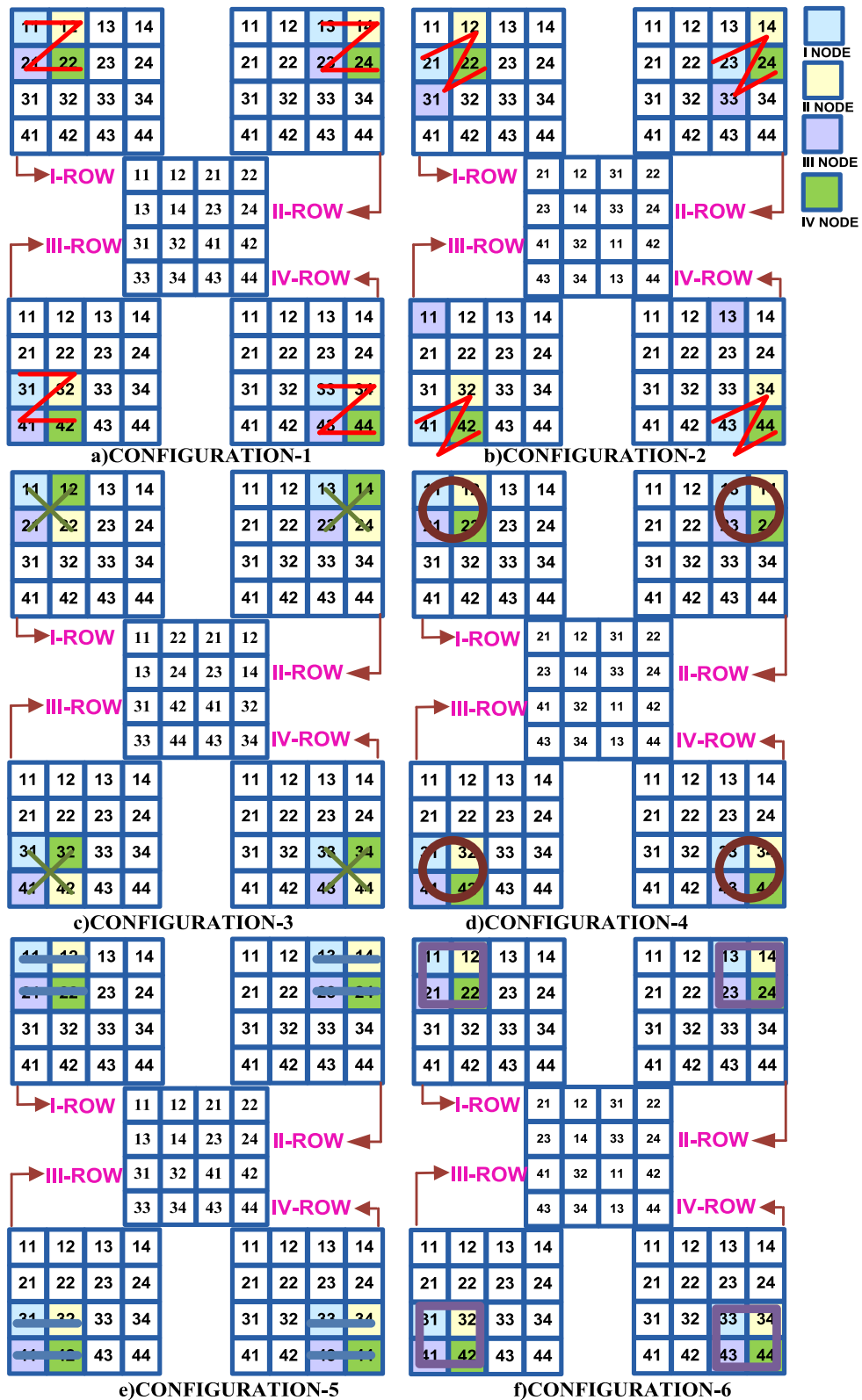


Figure-5. Shading pattern for an array configuration a) Configuration-1 b) Configuration-2 c) Configuration-3 d) Configuration-4 e) Configuration-5 f) Configuration-6.

Step 2. Find the row current for the array from I_1 to I_{mri} .

$$I_{mri} = \sum_{k=1}^m (G * I_m) / G_o$$

Step 3. Calculate mismatch loss for the PV array. The mismatch loss is the difference between maximum power developed from the module and the power developed from the module.

Step 4. Calculate Power loss which is the difference between maximum power developed from the PV array and the power developed from the module.

Step 5. Calculate Fill factor = $(V_m * I_m) / (V_{oc} * I_{sc})$

4. Different shading pattern

Fig. 4 shows the different shading patterns which solar PV arrays are subjected. The PV cells in the partially shaded region are physically moved to unshaded region to bring equal row current. The different configurations are shown in Figs. 5 and 14. The interconnections are modified as per the configuration and the power output from the PV arrays are measured.

Fig. 6 shows the MATLAB Simulink of the proposed work in normal conditions. All the PV cells are subjected to irradiance of 1000 W/m^2 and the P-V and V-I curves are shown in Fig. 7. The maximum power output from the PV array is 160W and the short circuit current I_{sc} is 2A.

a) Case-1 Diagonal and Long

In this case shown in Fig. 4 a the PV modules 11,12,21,22,43 and 44 modules are at standard irradiance of 1000 W/m^2 , 23,32 and 33 modules are subjected to partial shading condition with irradiance of 700 W/m^2 , 31,34 and 24 modules are in the irradiance level of 500 W/m^2 the remaining modules are in 300 W/m^2 . The PV modules are connected in 11 different types of configurations. Under partial shaded condition the output power of the PV module is 96 W. The maximum output power obtained under this partial shading condition is in configuration shown in 5. g and 5. h and provides lowest mismatch loss and Power loss of 60W and listed in Tables 3-5. Maximum power loss occurs in first, third to sixth configuration in Fig. 4 and maximum fill factor of 0.42 shown in Fig. 20 a. Under such irradiance condition the maximum output power obtained in 96W whereas the seventh and eighth configuration produces an output of 100W and it is shown in Fig. 8.

b) Case-II Short and long

The shading pattern shown in Fig. 4 b, for this module 11,12,21,22,43 and 44 modules are in irradiance level of 500 W/m^2 , 31,32,41 and 42 modules are in 300 W/m^2 whereas the remaining modules in standard irradiance condition. Lowest mismatch losses of 2W and power loss of 60W in eleventh configuration shown in Fig. 5 k are listed in Table 4. In this configuration the fill factor of 0.42 shown in Fig. 20 b. The maximum output power obtained is 100W and it is shown in Fig. 9, when compared to 64W in normal condition and it is listed in Table 3.

c) Case-III Inverse diagonal

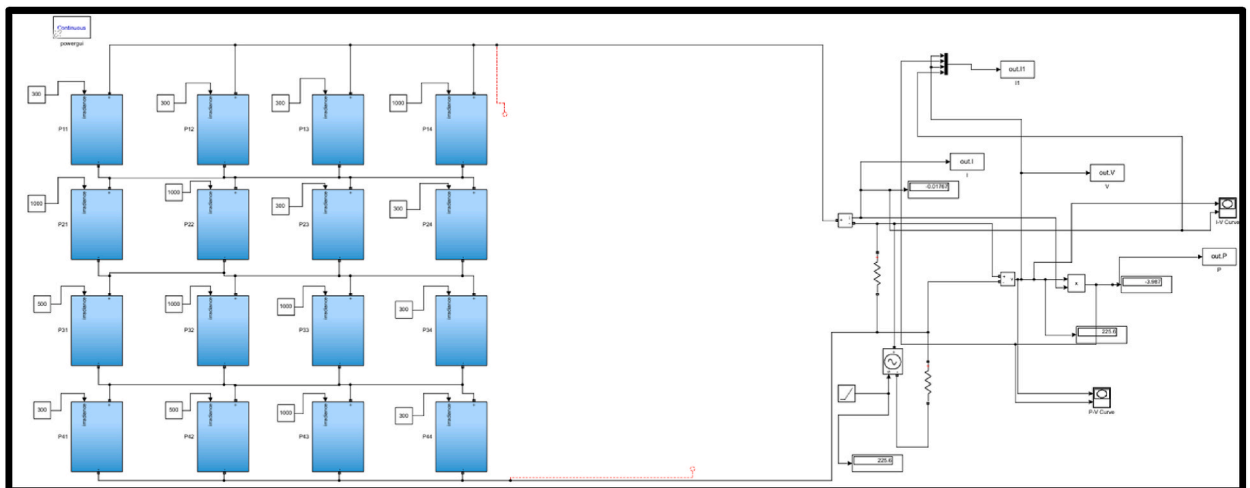


Figure-6. MATLAB simulink.

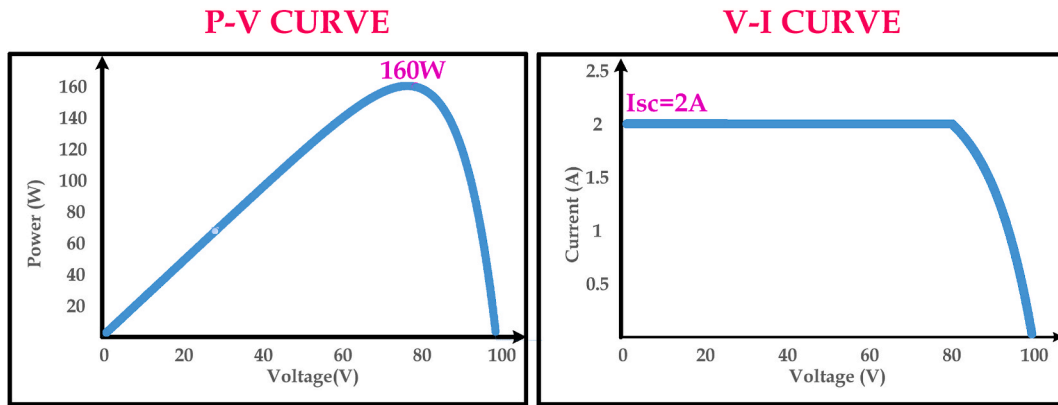


Figure-7. P-V & V-I curve for PV array under normal conditions.

The static configuration enhances output power of 16W in partial shaded condition than in normal condition and it is shown in Fig. 10 The shading pattern shown in Fig. 4 c has 300 W/m^2 irradiation in diagonal and the positions 21,31,32,41,42 and 43 are subjected to irradiance of 300 W/m^2 , whereas the remaining positions are at standard irradiation level. This configuration shown in Fig. 5 b has power loss of 88W with fill factor 0.30 and it is shown in Fig. 20 c.

d) Case-IV Short

With the reference of shading pattern in Fig. 4 d, the first row modules are subjected to 500 W/m^2 , the second row has irradiation level of 300 W/m^2 , the remaining modules in the PV array are in standard irradiance level. The configuration 7 and 11 shown in Fig. 5 g and 5. h enhance power output of 112 W under partial shaded conditions which is 2.33 times than the normal conditions shown in Fig. 11 and it is listed in Table 5. There is no mismatch losses in this configuration and power loss of 48W and fill factor of 0.4 shown in Fig. 20 d.

e) Case-V Long and short

In this case the shading pattern shown in Fig. 4 e has the last two columns are subjected to standard irradiance, first & second column of second and third row are subjected to 500 W/m^2 , whereas the remaining are subjected to irradiance level of 700 W/m^2 . The 10th and 11th configuration has $I_{sc} = 1.92 \text{ A}$, with output power of 128W shown in Fig. 12 PV curve and power loss of 32W and fill factor of 0.53 and it is listed in Table 5 and shown in Fig. 20 e.

f) Case-VI Inverse diagonal and long

The shading pattern has shown in Fig. 4 f which has an irradiation of 1000 W/m^2 in the left top corner and right bottom corner, 700 W/m^2 in the top and bottom corners whereas the modules are subjected to irradiation of 300 W/m^2 and 500 W/m^2 . The ninth configuration shown in 14. i has low mismatch losses of 4W when compared to other configurations and the characteristic curve is shown in Fig. 13. The Power loss is of 40W and fill factor of 0.5 in this configuration. The remaining configurations have power loss of 72W shown in Fig. 20 f. The mismatch loss and power losses for different configurations are listed in Table 5.

g) Case-VII Inverse short and long

The shading pattern is shown in Fig. 4 g. Maximum power from the module is obtained in 8th and 9th configuration shown in 14. h and 14. i has output power of 84W which is 1.5 times than in normal conditions. This configuration has low mismatch losses of 2W with fill factor of 0.35. The configurations like 1,3,4,5 and 6 have minimum fill factor of 0.20 which is shown in Fig. 20 g. The P-V and V-I characteristics of this shading pattern is shown in Fig. 15.

h) Case-VIII Diagonal

The shading pattern shown in 4. h has 500 W/m^2 in the diagonal and the below the modules are in the irradiation level of 300 W/m^2 . The maximum output power is obtained in the second configuration when compared with all the remaining configurations. The same power is obtained during normal conditions as well as partial shaded conditions shown in Fig. 20 h. The characteristic curve is shown in Fig. 16.

i) Case-IX Inverse long and diagonal

Table 4
Comparative analysis of Mismatch loss, Power loss and Fill factor of the proposed work.

CONFIG	DIAGONAL AND LONG			SHORT AND LONG			INVERSE DIAGNOL			SHORT		
	ML	PL	FF	ML	PL	FF	ML	PL	FF	ML	PL	FF
Normal	12	64	0.4	38	96	0.27	25	104	0.23	64	112	0.20
1	36	88	0.3	54	112	0.2	25	104	0.23	48	96	0.26
2	20	72	0.37	46	104	0.24	9	88	0.30	28	76	0.35
3	36	88	0.3	54	112	0.2	25	104	0.23	48	96	0.26
4	36	88	0.3	54	112	0.2	25	104	0.23	48	96	0.26
5	36	88	0.3	54	112	0.2	25	104	0.23	48	96	0.26
6	36	88	0.3	54	112	0.2	25	104	0.23	48	96	0.26
7	24	76	0.35	10	68	0.39	25	104	0.23	0	48	0.47
8	8	60	0.42	10	68	0.39	25	104	0.23	20	68	0.38
9	8	60	0.42	10	68	0.39	17	96	0.26	20	68	0.38
10	24	76	0.35	10	68	0.39	25	104	0.23	0	48	0.47
11	28	80	0.34	2	60	0.42	33	112	0.20	28	76	0.35
	LONG SHORT AND			INVERSE DIAGNOL AND LONG			INVERSE SHORT AND LONG			DIAGNOL		
	ML	PL	FF	ML	PL	FF	ML	PL	FF	ML	PL	FF
Normal	8	40	0.50	12	48	0.47	30	104	0.23	7	48	0.47
1	32	64	0.40	36	72	0.36	38	112	0.20	27	68	0.38
2	40	72	0.36	24	60	0.42	30	104	0.23	7	48	0.47
3	32	64	0.40	36	72	0.36	38	112	0.20	27	68	0.38
4	32	64	0.40	36	72	0.36	38	112	0.20	27	68	0.38
5	32	64	0.40	36	72	0.36	38	112	0.20	27	68	0.38
6	32	64	0.40	36	72	0.36	38	112	0.20	27	68	0.38
7	0	32	0.53	24	60	0.42	30	104	0.23	27	68	0.38
8	20	52	0.45	20	56	0.43	2	76	0.35	15	56	0.43
9	20	52	0.45	4	40	0.50	2	76	0.35	35	76	0.35
10	0	32	0.53	12	48	0.47	30	104	0.23	27	68	0.38
11	0	32	0.53	36	72	0.36	10	84	0.31	39	80	0.33
	INVERSE DIAGNOL AND LONG			INVERSE SHORT AND LONG			INVERSE SHORT			CENTRE		
	ML	PL	FF	ML	PL	FF	ML	PL	FF	ML	PL	FF
Normal	8	40	0.5	34	96	0.26	64	112	0.20	24	48	0.47
1	40	72	0.36	50	112	0.20	48	96	0.26	4	28	0.55
2	20	52	0.45	42	104	0.23	20	68	0.38	16	40	0.50
3	40	72	0.36	50	112	0.20	48	96	0.26	4	28	0.55
4	40	72	0.36	50	112	0.20	48	96	0.26	4	28	0.55
5	40	72	0.36	50	112	0.20	48	96	0.26	4	28	0.55
6	40	72	0.36	50	112	0.20	48	96	0.26	4	28	0.55
7	12	44	0.48	14	76	0.35	0	48	0.47	24	48	0.47
8	8	40	0.50	14	76	0.35	28	76	0.35	24	48	0.47
9	8	40	0.50	14	76	0.35	28	76	0.35	24	48	0.47
10	0	32	0.53	14	76	0.35	0	48	0.47	24	48	0.47
11	32	64	0.40	22	84	0.31	20	68	0.38	24	48	0.47
	DOUBLE LADDER			L CORNER			COLUMN LEFT			TWO CORNER		
	ML	PL	FF	ML	PL	FF	ML	PL	FF	ML	PL	FF
Normal	8	60	0.42	45	112	0.20	0	60	0.42	8	56	0.43
1	28	80	0.33	37	104	0.23	36	96	0.26	64	112	0.20
2	8	60	0.42	29	96	0.26	36	96	0.26	36	84	0.31
3	28	80	0.33	37	104	0.23	36	96	0.26	64	112	0.20
4	28	80	0.33	37	104	0.23	36	96	0.26	64	112	0.20
5	28	80	0.33	37	104	0.23	36	96	0.26	64	112	0.20
6	28	80	0.33	37	104	0.23	36	96	0.26	64	112	0.20
7	20	72	0.36	9	76	0.35	0	60	0.42	28	76	0.35
8	12	64	0.40	37	104	0.23	20	80	0.33	0	48	0.47
9	12	64	0.40	37	104	0.23	28	88	0.30	0	48	0.47
10	12	64	0.40	9	76	0.35	0	60	0.42	0	48	0.47
11	28	80	0.33	29	96	0.26	0	60	0.42	48	96	0.26
	ONE CORNER			RANDOM TWO CORNER								
	ML	PL	FF	ML	PL	FF						
	19	48	0.47	4	48	0.47						
1	67	96	0.26	44	88	0.30						
2	47	76	0.35	24	68	0.38						
3	67	96	0.26	44	88	0.30						
4	67	96	0.26	44	88	0.30						
5	67	96	0.26	44	88	0.30						
6	67	96	0.26	44	88	0.30						
7	19	48	0.47	12	56	0.43						
8	19	48	0.47	4	48	0.47						

(continued on next page)

Table 4 (continued)

CONFIG	DIAGONAL AND LONG			SHORT AND LONG			INVERSE DIAGNOL			SHORT		
	ML	PL	FF	ML	PL	FF	ML	PL	FF	ML	PL	FF
9	39	68	0.38	4	48	0.47						
10	19	48	0.47	12	56	0.43						
11	19	48	0.47	52	96	0.26						

Table 5

Comparison of Shading pattern for different configurations.

Shading Pattern	a	b	c	d	e	f	g	h	i	j	k	l	m	n	o	p	q	r	P _{max} in Total no of configuration
1.											✓								1
2.			✓					✓				✓							3
3.											✓								1
4.											✓								1
5.											✓								1
6.											✓								1
7.				✓					✓	✓			✓	✓	✓		✓		7
8.	✓							✓		✓						✓	✓	✓	6
9.	✓							✓		✓						✓	✓	✓	6
10.				✓	✓			✓		✓			✓	✓	✓	✓	✓	✓	10
11.		✓			✓											✓	✓		4

✓- Maximum output power under particular partial shading condition and particular configuration.

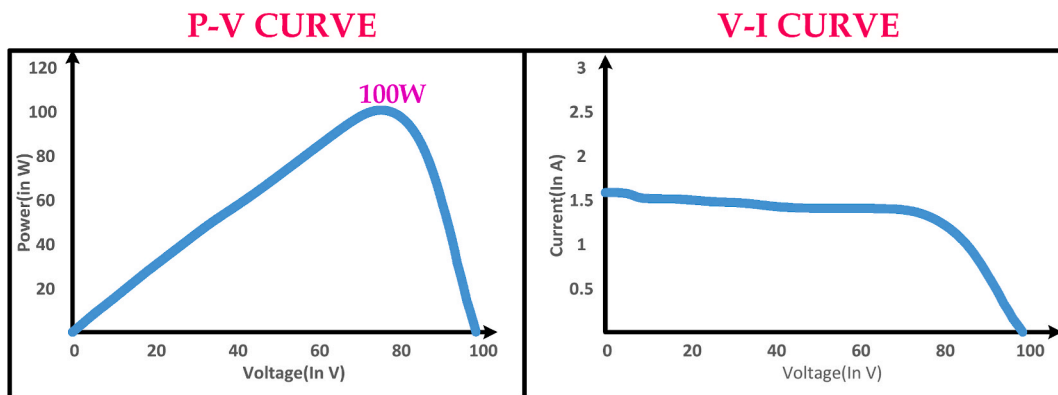


Figure-8. P-V & V-I curve for PV array under diagonal and long shading conditions.

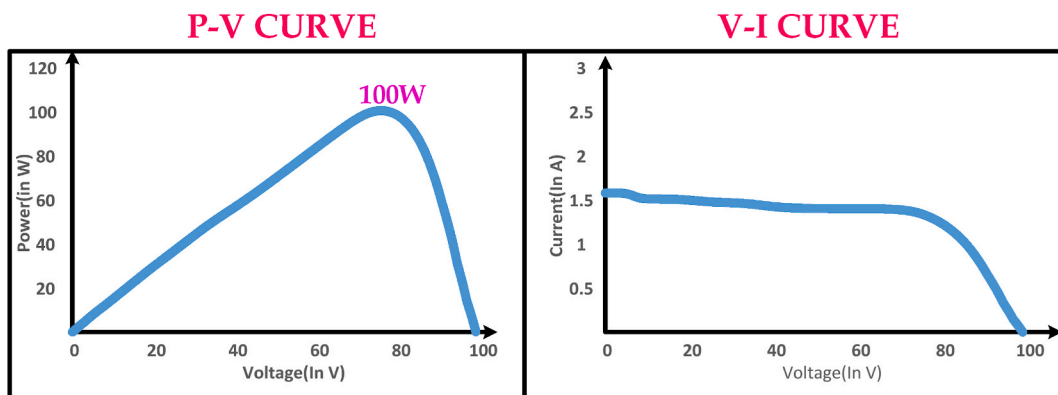


Figure-9. P-V & V-I curve for PV array under short and long shading conditions.

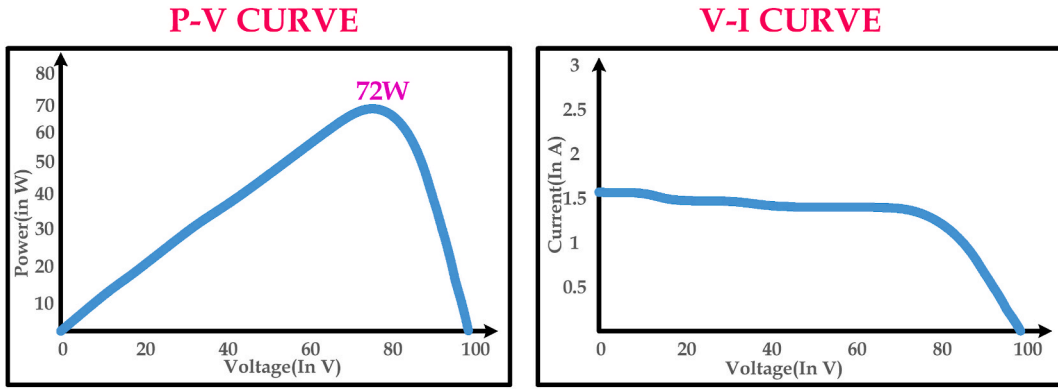


Figure-10. P-V & V-I curve for PV array under inverse diagonal shading conditions.

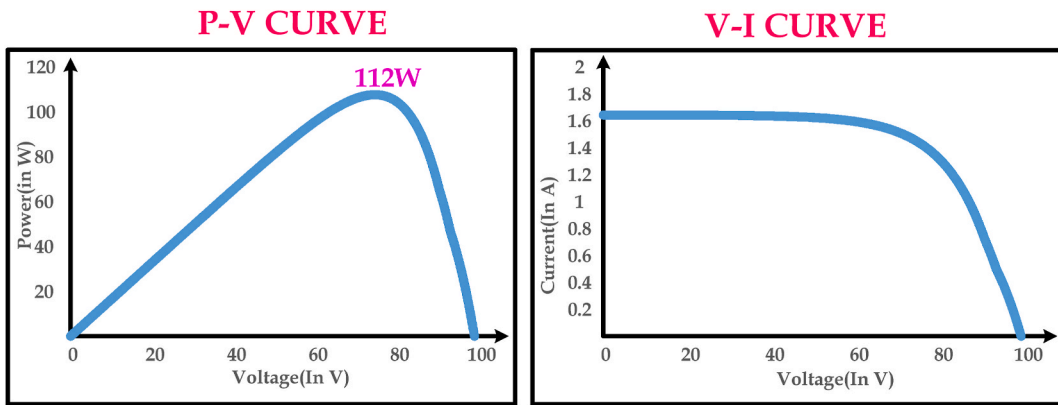


Figure-11. P-V & V-I curve for PV array under short shading conditions.

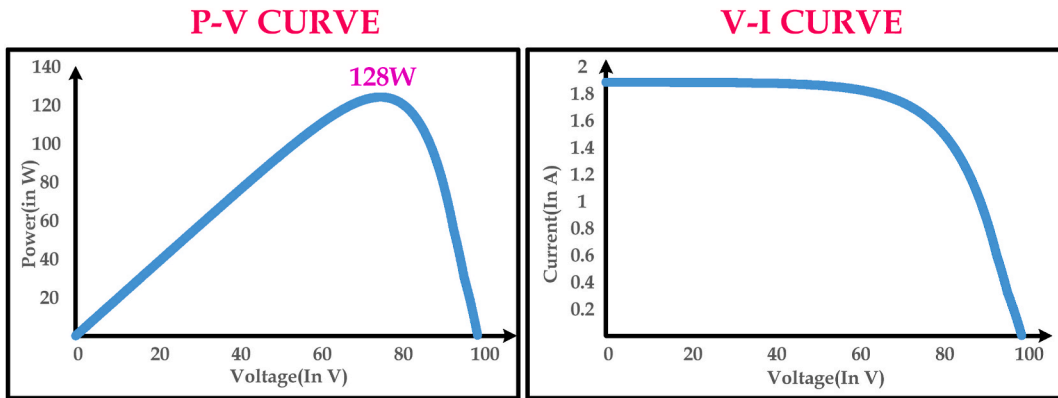


Figure-12. P-V & V-I curve for PV array under long and short shading conditions.

The shading pattern in Fig. 4 i has standard irradiance in left top corner and right bottom corner. the modules 13,14,24 and 32 is subjected to irradiance of 700 W/m^2 , theremaining modules are in 500 W/m^2 . The configuration shown in Fig. 20 h has 1.06 times of output power in partial shaded condition than in normal condition with zero power loss with fill factor of 0.53.128W of maximum output power is obtained in this configuration and it is shown in Fig. 17 with short circuit current of 1.8A.

j) Case-X Inverse long and short

The shading pattern shown in 4. j has 300 W/m^2 and 1000 W/m^2 in the left and right sides of first three rows. Left columns of fourth

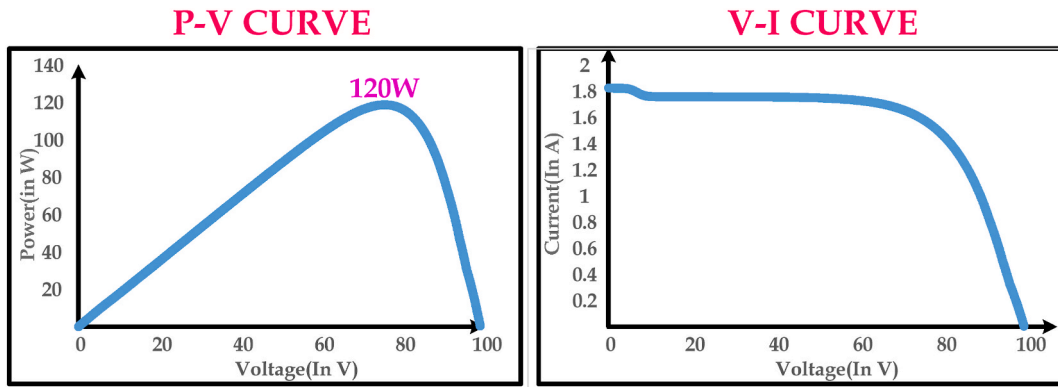


Figure-13. P-V & V-I curve for PV array under Inverse diagonal and long shading conditions.

row is subjected to irradiance of $500\text{W}/\text{m}^2$. Static configuration pattern of 7th, 8th, 9th and 10th in PV module results in 2.33 times of output power in partial shaded conditions than in normal conditions with fill factor 0.35 shown in Fig. 20 i and listed in Table 5. The curve is plotted between power and voltage, voltage and current and shown in Fig. 18.

k) Case XI Inverse Short

In the shading pattern shown in Fig. 4 k, the last rows are at standard irradiance level where as the second and first rows are in the irradiance level of $500\text{W}/\text{m}^2$ and $300\text{W}/\text{m}^2$ respectively. Fig. 5 k shows that the 7th and 10th configuration interconnection produce maximum output power in partial shaded condition and it is shown in Fig. 19. This is 2.33 times than in normal condition with zero mismatch losses and power loss of 48W and it is shown in Fig. 20 j.

l) Case XII Centre

The shading pattern is shown in Fig. 4 l. The modules 22 and 32 are subjected to irradiance level of $300\text{W}/\text{m}^2$ and 23 and 33 modules are at $500\text{W}/\text{m}^2$. The remaining modules are in standard irradiance conditions. Configurations like 1st, 3rd, 4th and 5th results maximum power output of 132 W and it shown in Fig. 21 k with power loss of 28W and fill factor of 0.55.

m) Case XIII Double ladder

The shading pattern resembles like double ladder type and it is illustrated in Fig. 4 m. The shading pattern in 1st&2nd configuration results short circuit current of 1.5A and output power of 100W with fill factor of 0.42 with 8W power as mismatch losses shown in 21. m. The output power in normal condition is same as in partial shading condition and it is listed in Table 5.

n) Case XIV L-Corner

With reference to the shading pattern shown in Fig. 4 n, the modules in the corner at lowest irradiance level of $300\text{W}/\text{m}^2$. Configurations like 7 and 10 provide maximum power of 84W in partial shaded conditions when compared to 48W in normal conditions and it is listed in Table 3 and shown in Fig. 21 n. The configuration has power loss of 76W with fill factor of 0.35.

o) Case XV Column left

The shading pattern shown in Fig. 4 o has decreasing order of irradiation towards left. The configurations 7th, 10th and 11th has I_{SC} of 1.5 A with same output power in partial shaded condition than in normal with no mismatch losses and fill factor of 0.42 is shown in Fig. 21 o.

p) Case XVI Two Corner

The shading pattern is shown in Fig. 4 p and the standard irradiance conditions are in top left corner and bottom right corner, $300\text{W}/\text{m}^2$ in top right corner and $500\text{W}/\text{m}^2$ in bottom left corner. Three configurations 8th, 9th and 10th configurations have zero mismatch losses and no mismatch losses is shown in Fig. 21 p and have I_{SC} of 1.68A and power loss of 48W with fill factor of 0.47.

q) Case XVII One Corner

The shading pattern in Fig. 4 q consists of first two columns and first rows are subjected to standard irradiance level, the subsequent

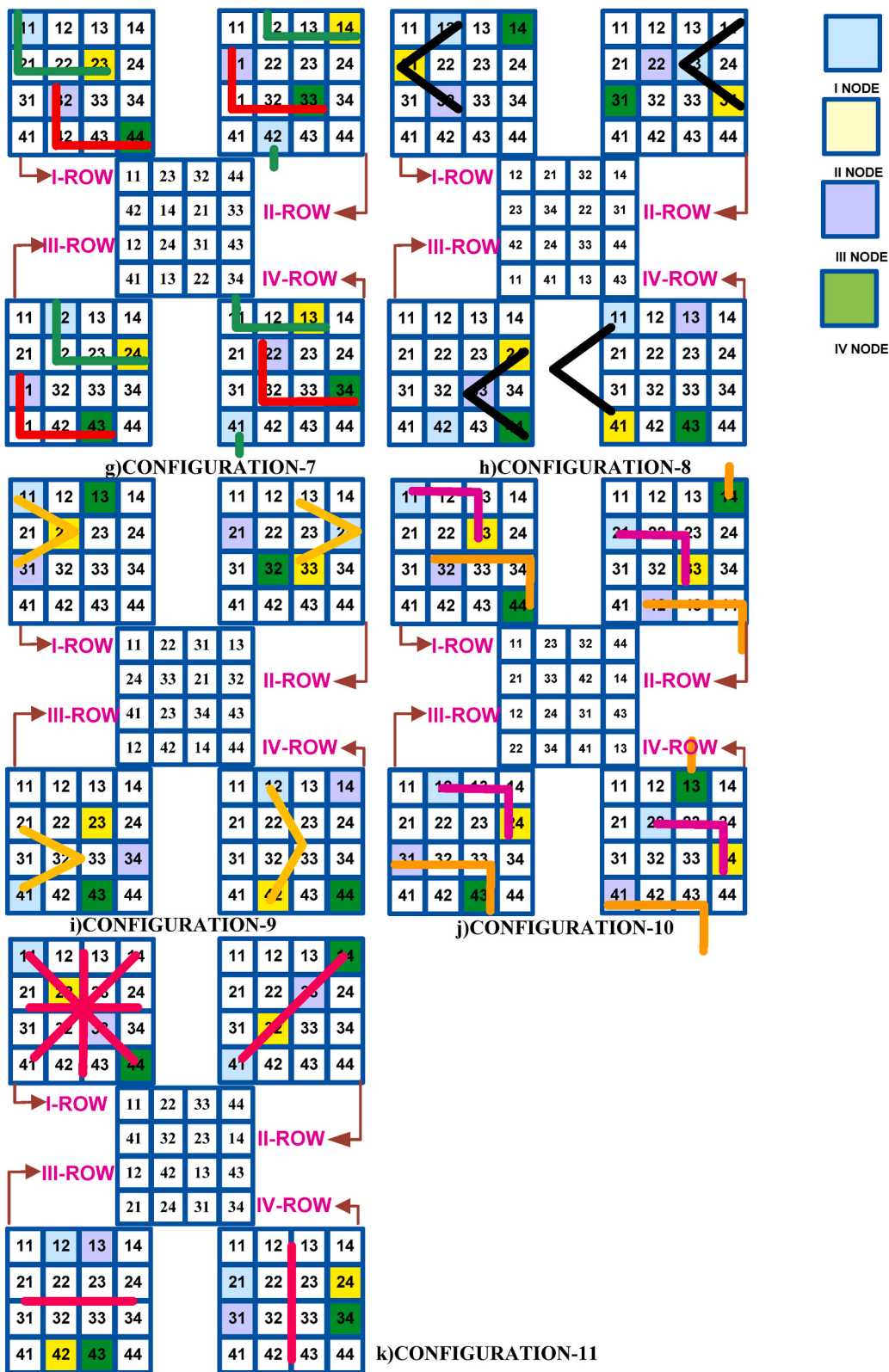


Figure-14. Shading pattern for an array configuration g) Configuration-7 h) Configuration-8 i) Configuration-9 j) Configuration-10 k) Configuration-11.

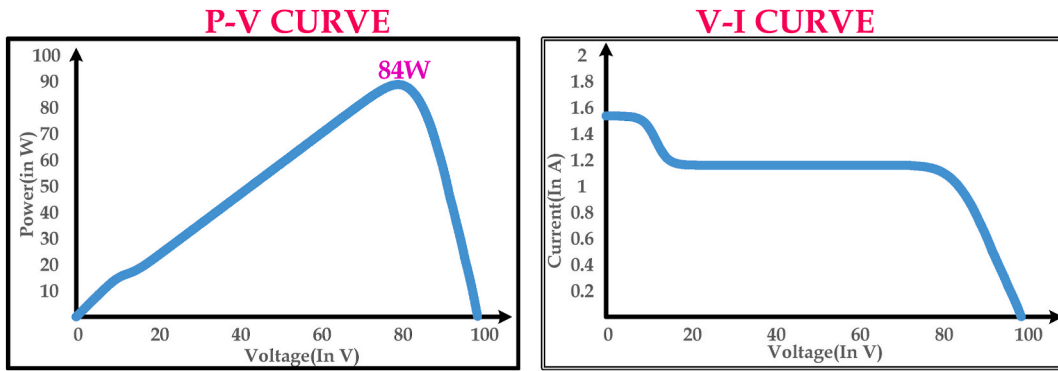


Figure-15. P-V & V-I curve for PV array under Inverse short and long shading conditions.

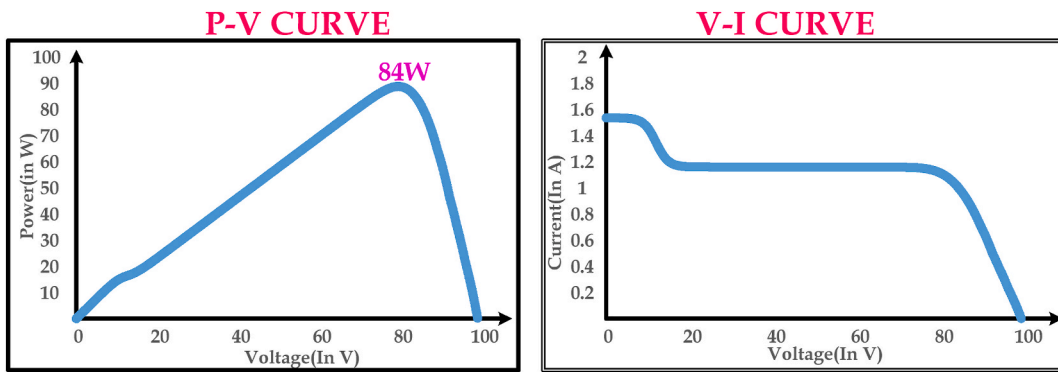


Figure-16. P-V & V-I curve for PV array under diagonal shading conditions.

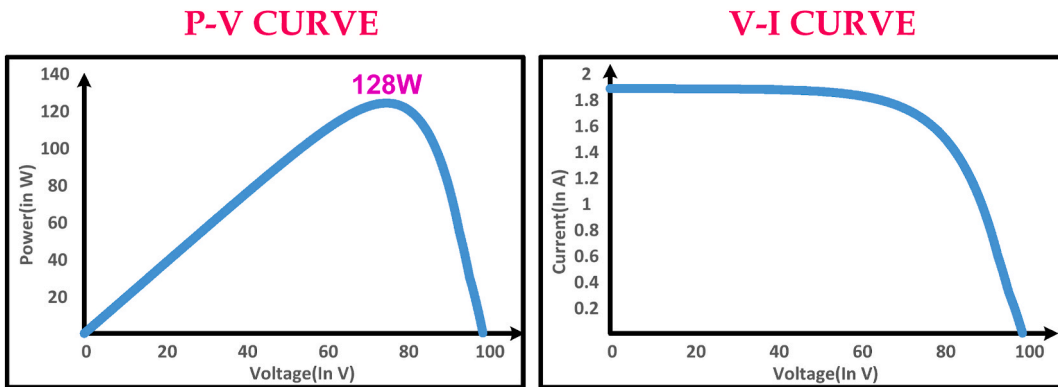


Figure-17. P-V & V-I curve for PV array under inverse long and diagonal shading conditions.

levels of third and fourth columns are at irradiance level of 500W/m^2 and 300W/m^2 . Configurations 7th,8th,10th and 11th configurations results in maximum power output of 112W with minimum mismatch losses and power loss of 19W with fill factor of 0.47. This is shown in Fig. 21 q.

r) Case XVIII Random two corner

In this shading pattern in Fig. 5 r the top right corner and bottom left corner in irradiance of 1000W/m^2 , the modules 11th and 44th are in irradiance of 300W/m^2 while the remaining are in 500W/m^2 . This configuration results in increase of output power of 112W with power loss of 48W with fill factor of 0.47 shown in Fig. 20 r.

Table 4 lists the comparison of maximum power output from different configurations under different partial shading conditions.

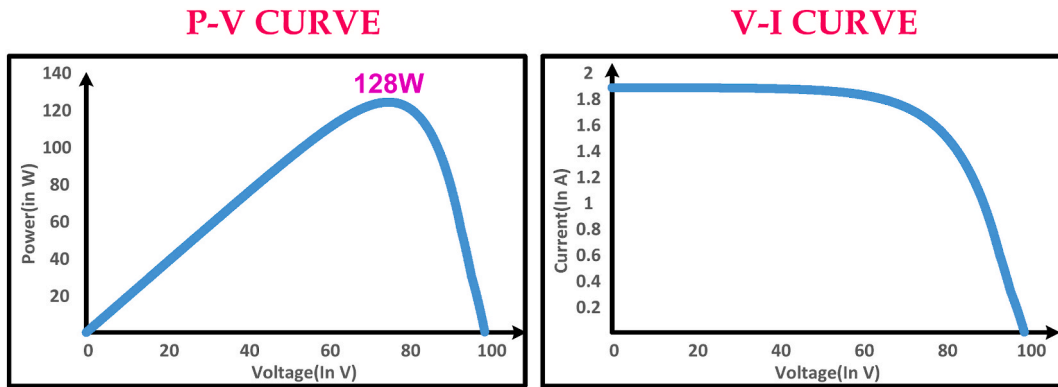


Figure-18. P-V & V-I curve for PV array under inverse long and short shading conditions.

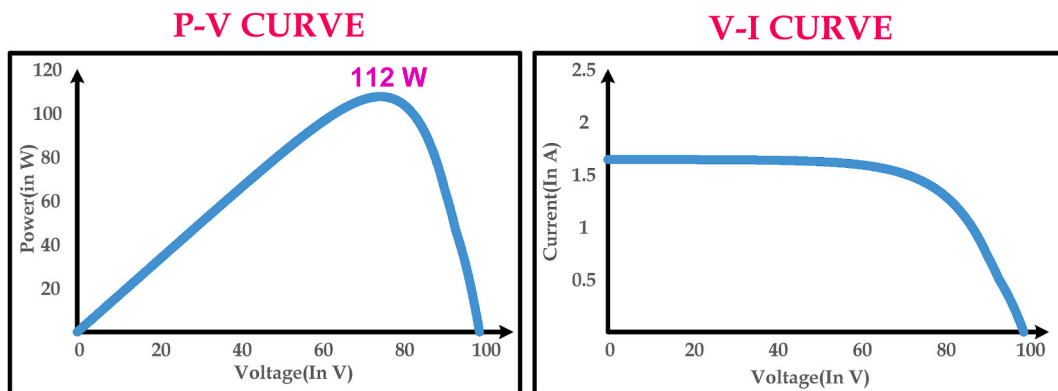


Figure-19. P-V & V-I curve for PV array under inverse short shading conditions.

Under 18 different partial shading conditions, the tenth configuration shown in Fig. 14 j provides maximum power output with low mismatch and power loss when compared to other configurations. The seventh configurations shown in Fig. 14 g provides maximum power output in 7 partial shaded conditions. Configurations 8th and 9th produces maximum output power in six different partial shaded conditions whereas the eleventh configuration has four. The remaining configurations produce maximum power only in one partial shaded condition.

5. Conclusion

This paper proposes different configurations for maximum power extraction from the PV arrays under different partial shaded conditions. An experimental analysis is carried for 4×4 PV arrays under different partial shading conditions with different configurations. For each configurations the output power from the array, power losses and mismatch losses are calculated. The comparison results provide the selection of suitable configurations under different shaded conditions for maximum power enhancement. For energy enhancement under partial shaded conditions, it is better to select the configuration with maximum power output under different shading pattern. The experimental results indicate that the PV arrays connected in configuration-10 have more power extraction when compared to other different configurations and it is suitable for large $m \times n$ PV arrays.

CRedit authorship contribution statement

Sakthivel Ganesan: Writing – original draft, Methodology, Investigation, Formal analysis, Data curation, Conceptualization. **Prince Winston David:** Writing – review & editing, Supervision, Software, Resources, Project administration, Methodology, Data curation, Conceptualization. **Praveen Kumar Balachandran:** Writing – original draft, Validation, Supervision, Software, Project administration, Funding acquisition, Data curation, Conceptualization. **Ilhami Colak:** Writing – review & editing, Visualization, Supervision, Resources, Project administration, Funding acquisition.

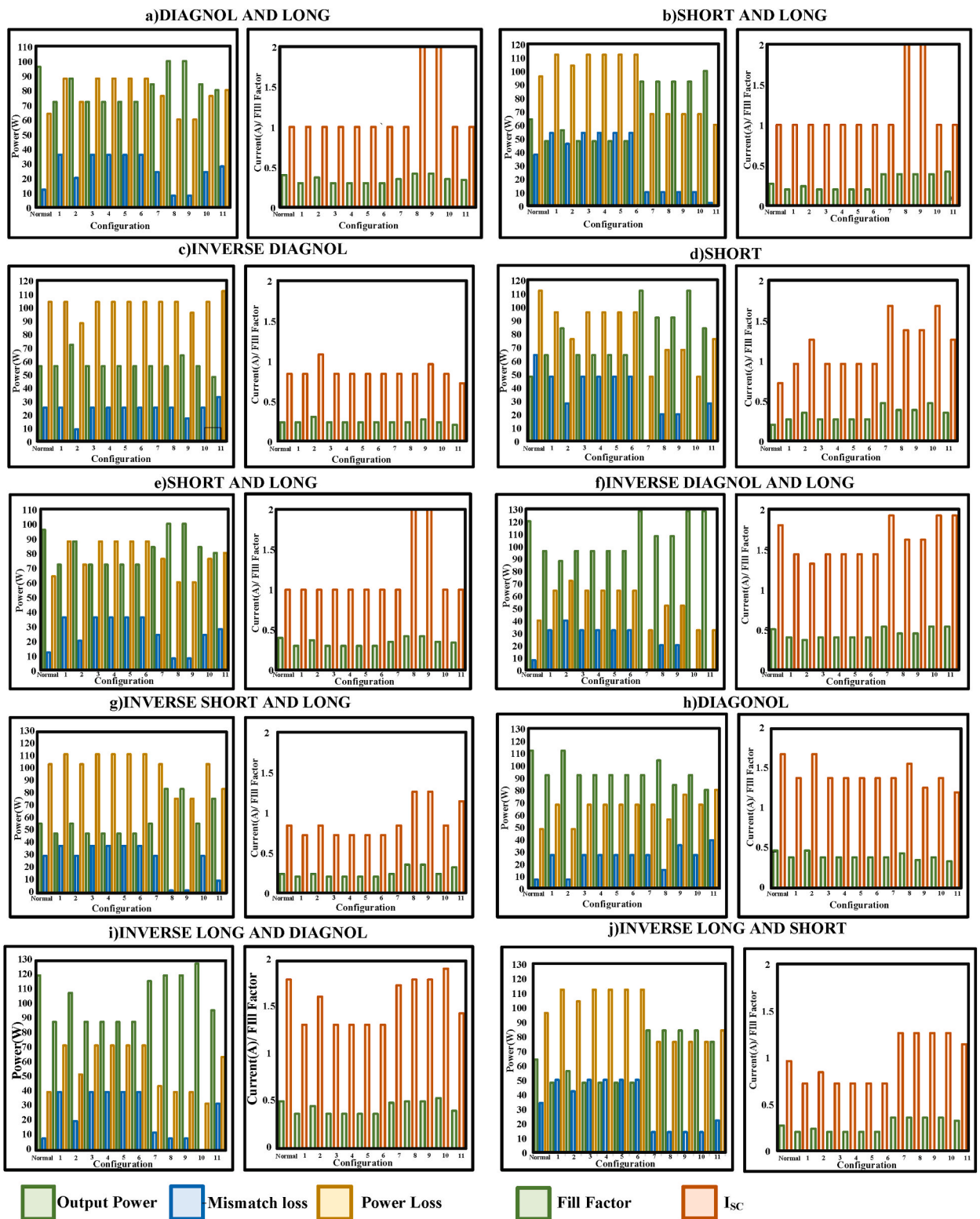


Figure-20. Parameters under different partial shading condition a) Diagonal and long b) Short and long c) Inverse diagonal d) short e) Short and long f) Inverse diagonal and long g) Inverse short and long h) Diagonal i) Inverse long and diagonal j) Inverse long and short.

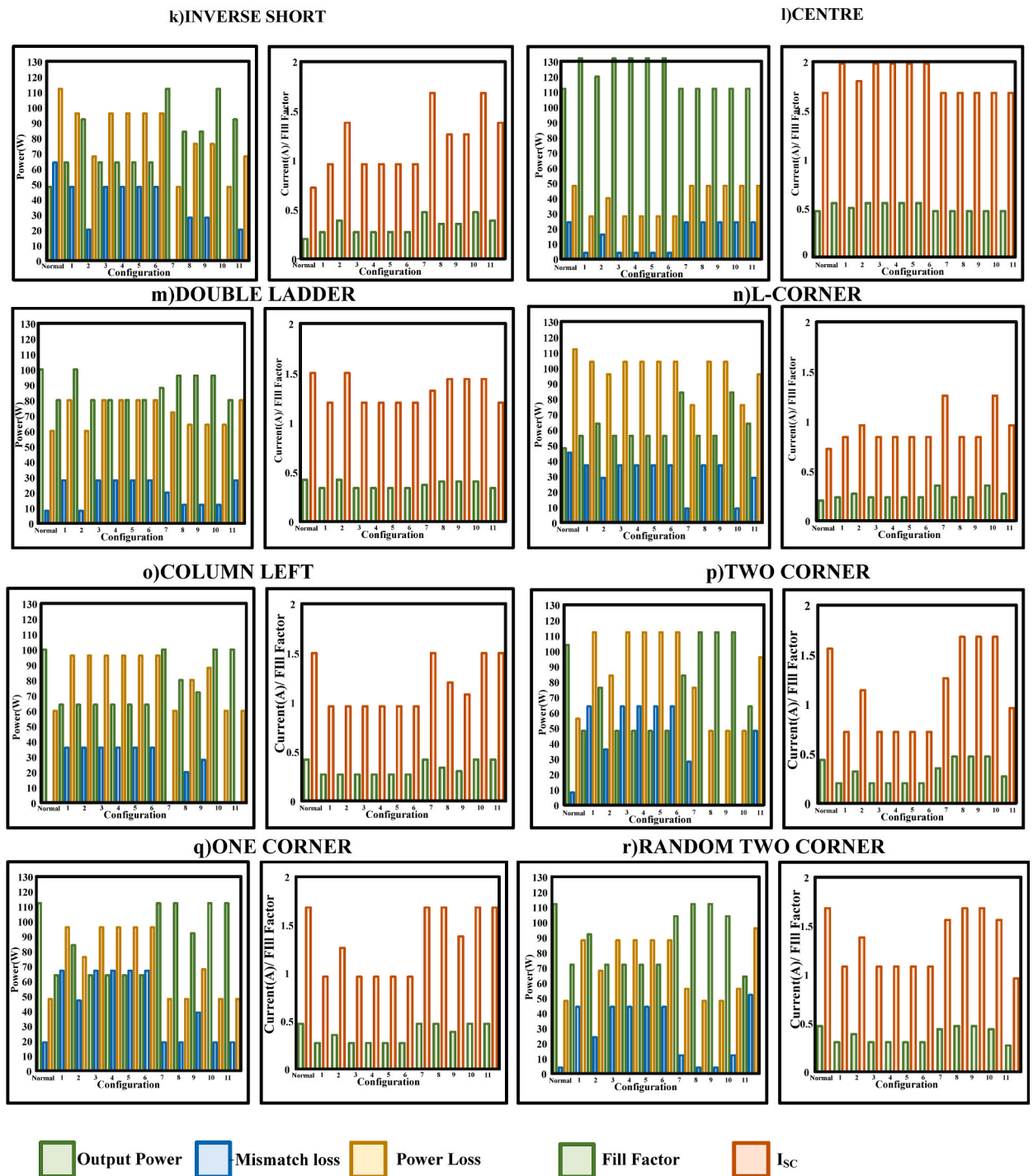


Figure-21. Parameters under different partial shading condition k)Inverse short l)centre m)Double ladder n) L-Corner o) Column left p)Two corner q)One corner r)Random two corner.

Declaration of competing interest

The authors declare that they have no known competing financial interests or personal relationships that could have appeared to influence the work reported in this paper.

References

- [1] M. Gul, Y. Kotak, T. Muneer, Review on recent trend of solar photovoltaic technology, *Energy Explor. Exploit.* 34 (4) (Jul. 2016) 485–526, <https://doi.org/10.1177/0144598716650552>.
- [2] M. Azharuddin Shamsuddin, T.S. Babu, T. Dragicevic, M. Miyatake, N. Rajasekar, Priority-based energy management technique for integration of solar PV, battery, and fuel cell systems in an autonomous DC microgrid, *Elec. Power Compon. Syst.* 45 (17) (Oct. 2017) 1881–1891, <https://doi.org/10.1080/15325008.2017.1378949>.
- [3] D. Youstri, T.S. Babu, S. Mirjalili, N. Rajasekar, M.A. Elaziz, A novel objective function with artificial ecosystem-based optimization for relieving the mismatching power loss of large-scale photovoltaic array, *Energy Convers. Manag.* 225 (Dec. 2020), <https://doi.org/10.1016/j.enconman.2020.113385>.
- [4] P. Manoharan, et al., Improved Perturb and observation maximum power point tracking technique for solar photovoltaic power generation systems, *IEEE Syst. J.* 15 (2) (Jun. 2021) 3024–3035, <https://doi.org/10.1109/JSYST.2020.3003255>.
- [5] W.C. Sinke, Development of photovoltaic technologies for global impact, *Renew. Energy* 138 (Aug. 2019) 911–914, <https://doi.org/10.1016/j.renene.2019.02.030>.
- [6] D. Youstri, T.S. Babu, D. Allam, V.K. Ramachandaramurthy, E. Beshr, M.B. Eteiba, Fractional chaos maps with flower pollination algorithm for partial shading mitigation of photovoltaic systems, *Energies* 12 (18) (Sep. 2019), <https://doi.org/10.3390/en12183548>.
- [7] R. Ramaprabha, B.L. Mathur, A comprehensive review and analysis of solar photovoltaic array configurations under partial shaded conditions, *Int. J. Photoenergy* 2012 (2012), <https://doi.org/10.1155/2012/120214>. Hindawi Limited.
- [8] S. Ganesan, P.W. David, P.K. Balachandran, T. Senjyu, Fault identification scheme for solar photovoltaic array in bridge and honeycomb configuration, *Electr. Eng. (Aug. 2023)*, <https://doi.org/10.1007/s00202-023-01816-4>.
- [9] S. Ganesan, P.W. David, P. Murugesan, P.K. Balachandran, Solar photovoltaic system performance improvement using a new fault identification technique, *Elec. Power Compon. Syst.* (2023), <https://doi.org/10.1080/15325008.2023.2237013>.
- [10] S. Suriya kala, D. Prince winston, M. Pravin, G. Sakthivel, Maximum power enhancement in solar PV modules through modified TCT interconnection method, *Sustain. Energy Technol. Assessments* 60 (Dec. 2023) 103462, <https://doi.org/10.1016/j.seta.2023.103462>.
- [11] A.M. Ajmal, T. Sudhakar Babu, V.K. Ramachandaramurthy, D. Youstri, J.B. Ekanayake, Static and Dynamic Reconfiguration Approaches for Mitigation of Partial Shading Influence in Photovoltaic Arrays, 2023.
- [12] S. Rezaazadeh, A. Moradzadeh, K. Pourhossein, B. Mohammadi-Ivatloo, F.P. García Márquez, Photovoltaic array reconfiguration under partial shading conditions for maximum power extraction via knight's tour technique, *J Ambient IntellHumanizComput*, Sep. (2022), <https://doi.org/10.1007/s12652-022-03723-1>.
- [13] S.K. Soni, Madan mohan malaviya university of technology, north Dakota state university, institute of electrical and Electronics engineers. Uttar pradesh section, IEEE industry applications society, and institute of electrical and Electronics engineers, ICEE3-2020, in: *International Conference on Electrical and Electronics Engineering*, 2020. February 14-15.
- [14] G. Sai Krishna, T. Moger, Reconfiguration strategies for reducing partial shading effects in photovoltaic arrays: state of the art, *Sol. Energy* 182 (2019), <https://doi.org/10.1016/j.solener.2019.02.057>. Elsevier Ltd, pp. 429–452, Apr. 01.
- [15] P.D.S. Vicente, T.C. Pimenta, E.R. Ribeiro, Photovoltaic array reconfiguration strategy for maximization of energy production, *Int. J. Photoenergy* (2015) 2015, <https://doi.org/10.1155/2015/592383>.
- [16] A.I. Siddiq, H.N. Fadhel, M.O. Anwar, Automatic PV array reconfiguration under partial shading conditions, *Abdulrahman Ikram Siddiq /NTU Journal of Renewable Energy* 4 (1) (2023) 36–46, <https://doi.org/10.56286/ntujre.v4i1>.
- [17] T. Hariharasudhan, S. Suriyakala, W.D. Prince, P. Sathya, Dynamic and static reconfiguration analysis of solar PV array. <http://ymerdigital.com>.
- [18] N.K. Gautam, N.D. Kaushika, RELIABILITY EVALUATION OF SOLAR PHOTOVOLTAIC ARRAYS †, 2002 [Online]. Available: www.elsevier.com/locate/solener.
- [19] O. Bingöl, B. Özkaya, Analysis and comparison of different PV array configurations under partial shading conditions, *Sol. Energy* 160 (Jan. 2018) 336–343, <https://doi.org/10.1016/j.solener.2017.12.004>.
- [20] A. Srinivasan, et al., L-shape propagated array configuration with dynamic reconfiguration algorithm for enhancing energy conversion rate of partial shaded photovoltaic systems, *IEEE Access* 9 (2021) 97661–97674, <https://doi.org/10.1109/ACCESS.2021.3094736>.
- [21] S.K. Cherukuri, et al., Power enhancement in partial shaded photovoltaic system using spiral pattern array configuration scheme, *IEEE Access* 9 (2021) 123103–123116, <https://doi.org/10.1109/ACCESS.2021.3109248>.
- [22] P. Paul, S.K. Ghosh, K. Ghosh, D. Mukherjee, Analysis of Mismatch Losses Arising from Crystalline and Amorphous Silicon PV Panels, *An Indian Experience*, 2012.
- [23] H. Patel, V. Agarwal, MATLAB-based modeling to study the effects of partial shading on PV array characteristics, *IEEE Trans. Energy Convers.* 23 (1) (Mar. 2008) 302–310, <https://doi.org/10.1109/TEC.2007.914308>.
- [24] J.C. Teo, R.H.G. Tan, V.H. Mok, V.K. Ramachandaramurthy, C.K. Tan, Impact of bypass diode forward voltage on maximum power of a photovoltaic system under partial shading conditions, *Energy* 191 (Jan. 2020), <https://doi.org/10.1016/j.energy.2019.116491>.
- [25] M.A. Al Mamun, M. Hasanuzzaman, J. Selvaraj, Experimental investigation of the effect of partial shading on photovoltaic performance, *IET Renew. Power Gener.* 11 (7) (Jun. 2017) 912–921, <https://doi.org/10.1049/iet-rpg.2016.0902>.
- [26] V. Dalessandro, P. Guerriero, S. Daliento, A simple bipolar transistor-based bypass approach for photovoltaic modules, *IEEE J. Photovoltaics* 4 (1) (2014) 405–413, <https://doi.org/10.1109/JPHOTOV.2013.2282736>.
- [27] P. Guerriero, P. Tricoli, S. Daliento, A bypass circuit for avoiding the hot spot in PV modules, *Sol. Energy* 181 (Mar. 2019) 430–438, <https://doi.org/10.1016/j.solener.2019.02.010>.
- [28] D. Youstri, T.S. Babu, D. Allam, V.K. Ramachandaramurthy, E. Beshr, M.B. Eteiba, Fractional chaos maps with flower pollination algorithm for partial shading mitigation of photovoltaic systems, *Energies* 12 (18) (Sep. 2019), <https://doi.org/10.3390/en12183548>.
- [29] B.R. Peng, K.C. Ho, Y.H. Liu, A novel and fast MPPT method suitable for both fast changing and partially shaded conditions, *IEEE Trans. Ind. Electron.* 65 (4) (Apr. 2018) 3240–3251, <https://doi.org/10.1109/TIE.2017.2736484>.
- [30] K. Sangeetha, T. Sudhakar Babu, N. Rajasekar, Fireworks algorithm-based maximum power point tracking for uniform irradiation as well as under partial shading condition, in: *Advances in Intelligent Systems and Computing*, Springer Verlag, 2016, pp. 79–88, https://doi.org/10.1007/978-81-322-2656-7_8.